Analytical and Knowledge-Based Redundancy for Fault Diagnosis in Process Plants

Zohreh Fathi and W. Fred Ramirez
Dept. of Chemical Engineering, University of Colorado, Boulder, CO 80309

Jozef Korbicz
Dept. of Applied Mathematics and Computer Science, Higher College of Engineering, ul. Podgórna 50, 65-246, Zielona, Góra, Poland

The increasing complexity of process plants and their reliability have necessitated the development of more powerful methods for detecting and diagnosing process abnormalities. Among the underlying strategies, analytical redundancy and knowledge-based system techniques offer viable solutions. In this work we consider the adaptive inclusion of analytical redundancy models (state and parameter estimation modules) in the diagnostic reasoning loop of a knowledge-based system. This helps overcome the difficulties associated with each category. The design method is a new layered knowledge base that houses compiled/qualitative knowledge in the high levels and process-general estimation knowledge in the low levels of a hierarchical knowledge structure. The compiled knowledge is used to narrow the diagnostic search space and provide an effective way of employing estimation modules. The estimation-based methods that resort to fundamental analysis provide the rationale for a qualitatively-guided reasoning process. The overall structure of the fault detection and isolation system based on the combined strategy is discussed focusing on the model-based redundancy methods which create the low levels of the hierarchical knowledge base. The system has been implemented using the condensate-feedwater subsystem of a coal-fired power plant. Due to the highly nonlinear and mixed-mode nature of the power plant dynamics, the modified extended Kalman filter is used in designing local detection filters.

Introduction

The increasing complexity of process plants and a growing demand for fault-tolerance encourage industry to look for new and more powerful techniques for detecting and diagnosing process abnormalities. Over the years, many fault detection and diagnosis methods have been developed for dynamical systems. In general, the fault detection and isolation (FDI) methods can be classified into pattern recognition (for example, fault dictionaries), logic-based/information flow graphs (for example, fault trees, signed directed graphs), and estimation/analytical redundancy categories, and more recently the knowledge-based system and neural network approaches. Several survey articles have been given by Willsky (1976), Isermann (1984), Himmelblau (1986), Basseville (1988), Frank (1990), Gertler (1991), and Korbicz et al. (1991). More comprehensive sources are books by Himmelblau (1978), Pau (1981), Basseville and Benveniste (1986), and Patten et al. (1989).

Analytical redundancy fault detection and isolation schemes basically refer to signal processing techniques employing state estimation, parameter estimation, adaptive filtering, variable threshold logic, and statistical decision theory. The various methods using this approach can be traced back to a few basic concepts. Among these are: the detection filter (Jones, 1973), the innovation test using Kalman filters or Luenberger observers (Yoshimura et al., 1979; Watanabe and Himmelblau, 1982), the parity space approach (Gertler and Singer, 1990; Patton and Chen, 1991), and the parameter estimation technique (Isermann, 1984). Over the past two decades, the basic research on FDI using analytical redundancy has evolved considerably due to advancements in methods of mathematical

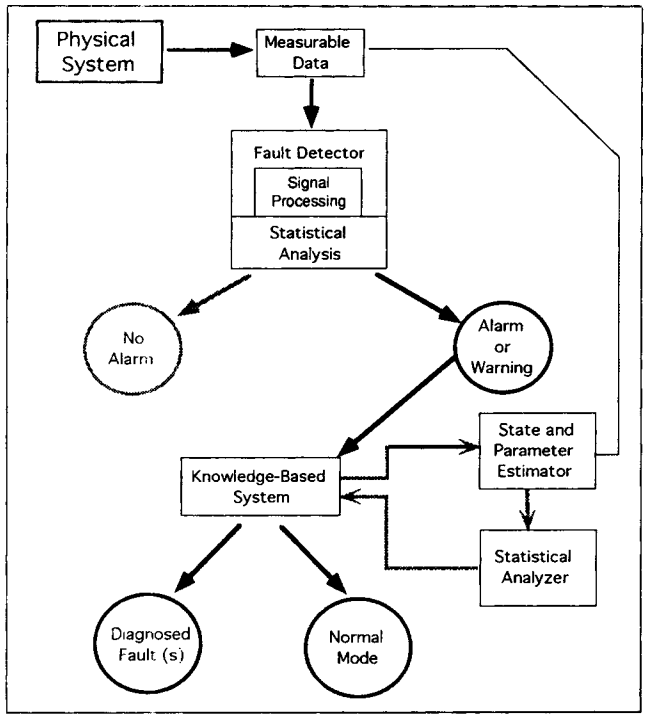

Figure 1. Overall block diagram of fault detection and diagnosis system.

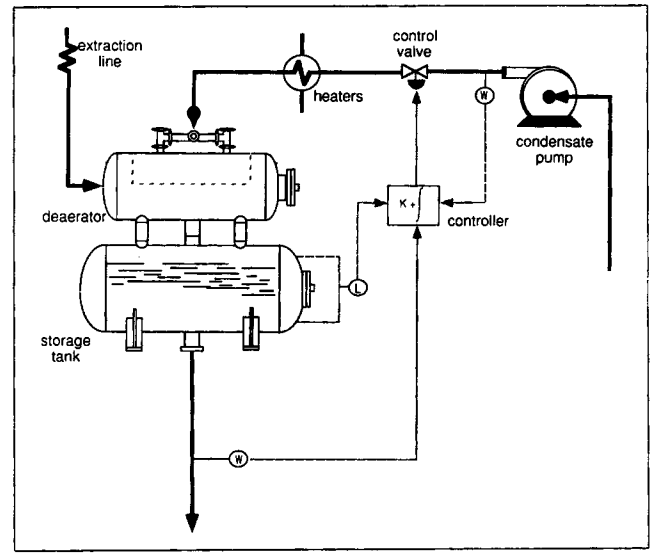

Figure 2. Condensate-feedwater subsystem.

modeling, state estimation, and parameter identification (Patton et al., 1989; Frank, 1992). However, the complexity and the prerequisites (for example, enough sensor information and appropriate, valid mathematical models) of this powerful systematic approach to FDI have precluded its widespread applications. In the last decade, reemergence of artificial intelligence has led to a knowledge-based system (Tzafestas, 1989) and neural network applications (Naidu et al., 1990; Yao and Zafiriou, 1990). These methods are especially interesting and important from a practical point of view and can complement the existing analytical and algorithmic methods of fault detection by application of artificial intelligence (Miller et al., 1990; Johannsen and Alty, 1991). The main advantage of a knowledge-based system approach lies in the fact that it makes use of qualitative models based on the available knowledge of the system. Common difficulties include lack of flexibility and reliability, ambiguity, and spurious solutions (Fathi et al., 1992). The combinations of both analytical and knowledge-based redundancy will allow the use of all available information given by numeric and symbolic models for performing the fault detection and diagnosis task and will alleviate the deficiencies associated with each approach.

This work considers an integrated approach based on combining the analytically-redundant FDI schemes and the knowledge-based techniques. The overall structure of our diagnostic methodology of embedding estimation-based techniques within the framework of a knowledge base is represented in Figure 1. The raw data are fed to a fault detector (a preprocessor) which performs statistical tests to identify the process condition (normal or abnormal). The preprocessor is basically an alarm system that is used to trigger the initiation of the knowledge-based system. The task of the knowledge base is to determine the source and extent of the true fault. Both a state/parameter estimator and a statistical analyzer are included in the loop of diagnostic reasoning. The design methodology is a hierarchical knowledge structure with compiled knowledge at higher levels of abstraction and analytical redundancy at lower levels of abstraction. This integrated approach reduces the computational complexity associated with functionally-redundant schemes and increases the effectiveness of the knowledge-based approach.

The knowledge-based redundancy issues have been addressed in detail in another article (Fathi et al., 1992). In this article, the main emphasis is placed upon the model-based redundancy problems. First, the deaerator control subsystem of a coal-fired power plant and its mathematical model are described. Then, the analytical redundancy and the design of local filters for state and parameter estimation are presented. Issues related to the knowledge base and system implementation are briefly addressed. Simulation results for the power plant subsystem illustrating the validity of the implemented filters are shown in the last section.

Process Description and Model Formulation

The process schematic shown in Figure 2 represents the plant components and flow paths selected for prototype diagnostic system development. This diagram shows the condensate pump, the control valve, the deaerator level controller, the extraction steam pipe, and the deaerator and its storage tank. It does not include the low-pressure feedwater heaters; they are represented only as a flow resistance between the control valve and the deaerator. The objective, in this work, is the analysis of problems associated with the deaerator, its control system, and the transportation lines.

The various components have been modeled through the use of Molecular Modeling System (MMS) documents obtained from the Energy and Power Research Institute (EPRI). The mathematical model for each component consists of conservation of mass, conservation of energy, fluid mechanics, and fluid properties evaluated from appropriate steam table calls. In the following, each component is briefly described and the

model equations needed for formulating the analytical redundancy modules are presented.

Pump

The condensate pump is a variable speed centrifugal pump and is driven by an electric motor. In this class of pumps, the pumping element which imparts kinetic energy to the pumped fluid rotates (various types of centrifugal pumps are distinguished by the direction of movement of the fluid with respect to the axis of rotation). The kinetic energy is then recovered as stored energy at a higher fluid outlet pressure. The primary assumptions used in modeling the pump are: quasi-steady-state pump performance, adiabatic operation, no reverse flow, and no cavitation.

Conservation of Mass. The quasi-steady-state mass conservation relation for the pump is given as

$$\omega_p = \omega_c \tag{1}$$

where
ω_p = mass-flow rate of water leaving pump, lb_m/h (kg/h)
ω_c = mass-flow rate of condensate water entering pump, lb_m/h (kg/h)

Conservation of Energy. The steady-state energy balance for an adiabatic pump is expressed as

$$h_p = h_c + 2{,}544.4\ J/\omega_c \tag{2}$$

where
h_p = enthalpy of water leaving pump, Btu/lb_m (kJ/kg)
h_c = enthalpy of condensate water entering pump, Btu/lb_m (kJ/kg)
J = power required by pump, hp (kW)

The constant in this equation is a conversion factor (Btu/hp·h).

Fluid Mechanics. The pump characteristics are based on normalized curves. The normalized head curve relates the ratio of the pump volumetric flow rate to the pump speed, to the ratio of the developed head to the square of pump speed,

$$Q_p/N = f_Q(\Delta H_p/N^2) \tag{3}$$

where
Q_p = pump volumetric flow rate, gpm (L/s)
N = pump speed, rpm
ΔH_p = pump developed head, ft (m) of water

The normalized horsepower curve relates the ratio of pump brake horse power to the cube of pump speed, to the ratio of the developed head to the square of the pump speed,

$$J/N^3 = f_J(\Delta H_p/N^2) \tag{4}$$

These curves represent the pump operation at all speeds.

The steady-state mechanical energy balance for the pump with the assumption of constant density yields

$$\Delta H_p = 144\ (P_p - P_c)/\rho_c \tag{5}$$

where
P_p = pressure of water leaving pump, psia (kPa)
P_c = pressure of condensate water entering pump, psia (kPa)
ρ_c = density of condensate water entering pump, lb_m/ft^3 (kg/m^3)

The mass-flow rate and the volumetric flow rate through the pump are related by

$$\omega_c = 8.02\rho_c Q_p \tag{6}$$

where the constant is a conversion factor [(ft^3/h)/gpm].

Fluid Properties. The density and temperature of water leaving the pump are obtained from steam tables,

$$\rho_p = f(P_p,\ h_p) \tag{7}$$

$$T_p = f(P_p,\ h_p) \tag{8}$$

where
ρ_p = density of water leaving pump, lb_m/ft^3 (kg/m^3)
T_p = temperature of water leaving pump, °F (°C)

Valve

The valve shown in the process schematic (Figure 1) is a globe valve used primarily for modulating to control the flow rate through the valve for maintaining the liquid level in the deaerator storage tank. In a globe valve, the fluid passes through a restricted opening and changes direction several times, imposing a pressure drop. The basic assumptions used in modeling the valve are quasi-steady-state, adiabatic, no seal leakage, and no reverse flow.

Conservation of Mass. The quasi-steady-state mass balance for the valve results in

$$\omega_v = \omega_p \tag{9}$$

where
ω_v = mass-flow rate of water leaving valve, lb_m/h (kg/h)

Conservation of Energy. Under quasi-steady-state assumption and no heat transfer, the energy balance reduces to

$$h_v = h_p \tag{10}$$

where
h_v = enthalpy of water leaving the valve, Btu/lb_m (kJ/kg)

Fluid Mechanics. On writing a steady-state mechanical energy balance for a constant density fluid and solving for the mass-flow rate, we have

$$\omega_p = C_v[\rho_{pv}(P_p - P_v) + \rho_{pv}^2 \Delta H_v/144]^{1/2} \tag{11}$$

where
C_v = valve conductance
P_v = pressure of water leaving valve, psia (kPa)
ΔH_v = difference in elevation between inlet and outlet, ft (m)
ρ_{pv} = average of upstream and downstream fluid densities, lb_m/ft^3 (kg/m^3)

Since the low-pressure heaters are only modeled as a flow resistance, the valve conductance can be combined with the flow conductance of the pipe associated with the heaters. Upon combining the valve conductance, C_v, and the pipe conductance, C_p, in series, the equivalent conductance is:

$$C_{eq} = 1/\sqrt{(1/C_v)^2 + (1/C_p)^2} \tag{12}$$

Valve Characteristics. The valve conductance, C_v, varies with valve stroke according to its inherent valve characteristics. All valves provide for any of three characteristics:

$$\begin{aligned} &1.\ \text{Equal Percentage} && C_v = \Upsilon^3 C_{v_{max}} \\ &2.\ \text{Linear} && C_v = \Upsilon C_{v_{max}} \\ &3.\ \text{Quick Opening} && C_v = (1 - e^{-10\Upsilon}) C_{v_{max}} \end{aligned} \tag{13}$$

where
Υ = valve position (fraction)
$C_{v_{max}}$ = valve maximum conductance

Fluid Properties. The density and temperature of leaving fluid are calculated as a function of pressure and enthalpy using steam tables,

$$\rho_v = f(P_v, h_v) \tag{14}$$

$$T_v = f(P_v, h_v) \tag{15}$$

where
ρ_v = density of water leaving valve, lb_m/ft^3 (kg/m^3)
T_v = temperature of water leaving valve, °F (°C)

Extraction pipe

This pipe is the interconnecting component between the turbine and the deaerator. The extraction steam flows through this pipe before entering the deaerator. The primary phenomenon to be modeled is pressure losses due to friction and elevation. The friction factor is a function of Reynolds number and pipe roughness. However, for a given pipe roughness and turbulent flow, the friction factor can be assumed constant. The basic assumptions used in developing the model are: quasi-steady-state, single-phase flow, fully-developed turbulent flow, and no reverse flow.

Conservation of Mass. Under quasi-steady-state assumption, the mass conservation relation is

$$\omega_e = \omega_s \tag{16}$$

where
ω_s = mass-flow rate of steam entering the pipe, lb_m/h (kg/h)
ω_e = mass-flow rate of steam leaving pipe, lb_m/h (kg/h)

Conservation of Energy. The steady-state energy balance with no heat loss is given as

$$h_e = h_s \tag{17}$$

where
h_s = enthalpy of steam entering pipe, Btu/lb_m (kJ/kg)
h_e = enthalpy of steam leaving pipe, Btu/lb_m (kJ/kg)

Fluid Mechanics. Using the quasi-steady-state assumption and replacing the fluid density by the average of the upstream and downstream values, the mechanical energy balance can be solved for the mass-flow rate as

$$\omega_e = C_f[\rho_{se}(P_s - P_e) + \rho_{se}^2 \Delta H_{se}/144]^{1/2} \tag{18}$$

where
C_f = flow conductance
P_s = pressure of steam entering pipe, psia (kPa)
P_e = pressure of steam leaving pipe, psia (kPa)
ΔH_{se} = elevation difference between upstream and downstream segments, ft (m)
ρ_{se} = average of downstream and upstream fluid densities, lb_m/ft^3 (kg/m^3)

Fluid Properties. Fluid properties are calculated from steam tables,

$$\rho_e = f(P_e, h_e) \tag{19}$$

$$T_e = f(P_e, h_e) \tag{20}$$

where
ρ_e = density of steam leaving pipe, lb_m/ft^3 (kg/m^3)
T_e = temperature of steam leaving pipe, °F (°C)

Deaerator

The deaerator subsystem is composed of a deaerator (an open feedwater heater) and its storage tank. Deaerators serve four major tasks: removal of noncondensable gases to prevent corrosion and scaling of boiler surfaces due to gases dissolved in the feedwater, heating of feedwater, provide feedwater storage, and are located to provide a substantial net positive suction head on the boiler feed pumps, preventing pump cavitation. The feedwater is heated by spraying into a steam space. Most of the gases are released at this point due to the higher solubility of gases in steam than in water. The remaining deaeration takes place in the stack of trays or baffles. Steam with a high concentration of dissolved gases is vented into the atmosphere (since the amount of vented steam is small, this effect is neglected). The heated and deaerated feedwater is then collected in a storage tank below the deaerating section. The two sections are connected by a downcomer carrying the feedwater downward and equalizers interconnecting the steam spaces of the two sections to maintain their pressures at virtually identical values. The storage tank generally maintains sufficient storage to allow the plant to withstand an interruption of the condensate. It also serves to provide surge protection for the boiler feed pumps. The water level in the storage tank is maintained at a desired set point through a control valve placed on the condensate flow section upstream from the deaerator.

The major phenomena simulated are: phase equilibrium, feedwater heating and deaeration, and elevation head. The basic assumptions in model development are: phase equilibrium between liquid and vapor phases, equal pressure in the deaerating section and the storage tank, and negligible noncondensable gas effects.

Conservation of Mass. For a fixed control volume, the mass conservation relation can be written as

$$\frac{d\rho_d}{dt} = (\omega_{d_{in}} - \omega_{d_{out}})/3{,}600\ V_t \tag{21}$$

where
ρ_d = bulk density over entire vessel, lb_m/ft^3 (kg/m^3)
$\omega_{d_{in}}$ = mass flow rate of feedwater and steam entering deaerator, lb_m/h (kg/h)
$\omega_{d_{out}}$ = mass flow rate of fluid leaving deaerator, lb_m/h (kg/h)
V_t = total volume of deaerating and storage tanks, ft^3 (m^3)

Conservation of Energy. For a fixed control volume with no heat transfer and negligible kinetic energy effects, the energy balance gives

$$\frac{du_d}{dt} = \left(\omega_{d_{in}} h_{d_{in}} - \omega_{d_{out}} h_{d_{out}} - 3{,}600\, V_t u_d \frac{d\rho_d}{dt}\right) \Big/ (3{,}600\, \rho_d V_t) \quad (22)$$

where

u_d = bulk specific internal energy, Btu/lb$_m$ (kJ/kg)
$h_{d_{in}}$ = enthalpy of feedwater and steam entering deaerator, Btu/lb$_m$ (kJ/kg)
$h_{d_{out}}$ = enthalpy of fluid leaving deaerator, Btu/lb$_m$ (kJ/kg)

Fluid Mechanics. The deaerator includes the effect of the elevation difference between the deaerator and the boiler feed pumps. Upon neglecting the frictional losses in the line from the deaerator to the boiler feed pumps, the quasi-steady-state mechanical energy balance reduces to

$$P_{bfps} = P_d + \rho_{d_{out}} \Delta H_{db}/144 \quad (23)$$

where

P_{bfps} = pressure at boiler feed pump suction, psia (kPa)
P_d = pressure in the deaerator, psia (kPa)
$\rho_{d_{out}}$ = density of fluid leaving deaerator, lb$_m$/ft^3 (kg/m^3)
ΔH_{db} = elevation drop from deaerator to boiler feed pump, ft (m)

Fluid Properties. The pressure in the deaerator is defined by the bulk density and specific internal energy through the implicit equation,

$$\rho_d^{-1} = f(h_d, P_d) \quad (24)$$

$$h_d = u_d + \gamma P_d \rho_d^{-1} \quad (25)$$

where f represents a steam table function and γ is a conversion factor equivalent to 0.1851 (Btu·in^2)/(lb$_f$·ft^3).

The saturation properties are evaluated as functions of the deaerator pressure, using steam tables

$$\begin{aligned} h_{d_{out}} &= f(P_d), \quad T_{d_{out}} = f(P_d) \\ \rho_{d_{out}} &= f(P_d), \quad \rho_f = f(P_d), \quad \rho_g = f(P_d) \end{aligned} \quad (26)$$

where

$T_{d_{out}}$ = temperature of fluid leaving deaerator, °F (°C)
ρ_f = density of saturated liquid, lb$_m$/ft^3 (kg/m^3)
ρ_g = density of saturated vapor, lb$_m$/ft^3 (kg/m^3)

Geometry Calculations. The water level in the deaerator is determined by a mass accounting in the deaerating and the storage sections,

$$L = D \frac{(\rho_d - \rho_g)}{(\rho_f - \rho_g)} (V_t/V_s) \quad (27)$$

where

L = liquid level, in. (mm)
D = diameter of storage tank, in. (mm)
V_s = volume of storage tank, ft^3 (m^3)

Controller

The deaerator level controller is a three-mode proportional-integral controller with antireset windup. The error signal for the three-mode level controller that is direct acting (the output increases with an increase in set point) is defined as

$$\epsilon = k_1 (L_s - L_m) + k_2 \omega_{d_{out}} - k_3 \omega_c \quad (28)$$
$$\text{←demand→} \qquad \text{←supply→}$$

where

ϵ = control error signal
L_s = deaerator level set point, in. (mm)
L_m = deaerator level measured, in. (mm)
ω_c = mass flow rate of condensate water, lb$_m$/h (kg/h)
k_1, k_2, k_3 = constant parameters

The proportional and integral actions on the error signal are expressed as

$$O_P = k_P \epsilon \quad (29)$$

$$\frac{dO_I}{dt} = k_I [\epsilon + k_a [\min(O_h - O_T, 0) + \max(O_l - O_T, 0)]] \quad (30)$$

where

O_P = proportional output (fraction)
k_P = proportional gain
O_I = integrator output (fraction)
k_I = integrator gain, s^{-1}
k_a = gain on antireset windup
O_T = unbounded controller output
O_h = higher limit on controller output
O_l = lower limit on controller output

The antireset windup is provided through a bias, proportional to the amount the output has exceeded the limit. This serves to drive the integral action onto the limit smoothly when the controller is in an antireset mode. The unbounded controller output is the sum of the proportional and integral actions (the actual output is the bounded O_T).

$$O_T = O_P + O_I \quad (31)$$

The input parameters for the above mathematical model are given in Table 1.

Analytical Redundancy

Most of the work considering the problem of FDI from the point of analytical redundancy proposes to use the Kalman filter in the stochastic case, and the Luenberger observer in the deterministic case. For example, Mehra and Peschon (1971) have shown how the innovation properties can be used for fault detection (tests of whiteness, mean, covariance, and chi-square). Willsky et al. (1974, 1975) considered a class of failure detection—estimation problems involving random jumps in state variables. The first technique, called the weighted sum squared residual method, uses the weighted sum of squared residuals of a Kalman filter, designed using the system model without jumps, to detect faults and an information compensation method (which increments the filter gains), to reestimate the appropriate states. The compensation performance was found not to be consistently good. The second method, called multiple hypothesis method, employs a bank of linear filters for each of the hypothesized fault modes, and uses conditional probabilities for the various hypotheses in the detection pro-

Table 1. Input Parameters

Parameter	Value	Units
C_f	8.840×10^5	
C_p	4.403×10^4	
C_{vmax}	1.044×10^5	
D	144	in.
h_f	81.7	Btu/lb_m
h_s	1,353.2	Btu/lb_m
k_1, k_2, k_3	1, 10^{-6}, 10^{-6}	
k_d	1.0	
k_f	0.05	
k_p	0.10	
L_s	120	in.
N	1,800	rpm
O_n	1.0	
O_t	0.0	
P_s	1.42	psia
P_v	142.2	psia
V_s	8,000	ft^3
V_t	9,980	ft^3
$w_{d_{max}}$	4.5×10^6	lb_m/hr
ΔH_{se}	0.0	ft
ΔH_t	0.0	ft
ρ_s	61.8	lb_m/ft^3
ρ_v	0.213	lb_m/ft^3
Polynomial coefficients a_j $(j=0,1,2,3)^*$ for $f_Q(\Delta H_t/N^2)$	0.2083×10^3, -0.2465×10^7 0.1009×10^{11}, -0.1390×10^{14}	
Polynomial coefficients a_j $(j=1,2,3)^*$ for $f_J(\Delta H_p/N^2)$	-0.6954×10^{-2}, 0.8250×10^2 -0.1914×10^6	

* A general polynomial of order n has the form $y = a_0 + a_1x + a_2x^2 + \ldots + a_nx^n$
SI conversion: mm = in. × 25.4; kJ/kg = Btu/lb × 2.33; kg = lb × 0.454; m = ft × 0.3048; $m^3 = ft^3 \times 0.0283$; kPa = psi × 6.89.

cedure. The performance cost of this method is the high complexity of the detection system. Another similar technique is the generalized likelihood ratio (GLR) method presented by Willsky and Jones (1974, 1976). GLR, which requires a normal mode Kalman filter and a growing number of correlation calculations for different hypothesized fault types and times, is appropriate for changes that can be modeled as additive effects. Chien and Adams (1976) devised a linear detection system from the concepts of Wald's sequential probability ratio test (Wald, 1941) and information feedback. The design criterion in the combined control and decision problem is the minimization of the mean detection time for specified false- and missed-alarm error probabilities. The detector of Yoshimura et al. (1979) that considers parametric failures is composed of a normal mode Kalman filter and an adaptive extended Kalman filter for estimating states and parameters under the failure mode. Park and Himmelblau (1983) also used an extended Kalman filter to detect parametric failures. A two-level identification strategy (an observer for the states and a least-squares estimator for the parameters) has been proposed by Watanabe and Himmelblau (1983a,b) for process models nonlinear in states but linear in coefficients. Halme and Selkainaho (1986) introduced the idea of partitioning the system into smaller submodels and applied an adaptive filtering-based method to detect sensor faults. The nonlinear state observer approaches of Hengy and Frank (1986) and Wunnenberg and Frank (1990) are the nonlinear local state observers for component fault detection. A multiple model nonlinear filtering technique for the detection of leaks in a heat exchanger process has been recently presented by Laparo et al. (1991).

In the cited work, the Kalman filter algorithm is employed in different ways to solve the problem. Here, we base the design of our detectors on two concepts: structural decomposition and adaptive Kalman filtering. That is, the plant structure is decomposed into units for which individual filters are designed. In general, the design of local filters can range from one incorporating most likely fault modes to one incorporating all possible ones. To cover a broader range of practical domains, the modified extended Kalman filter which is designed for the joint state and parameter estimation in systems with coupled slow and fast dynamics is considered (Fathi et al., 1991).

In this section, the failure detection of the deaerator control subsystem of a coal-fired power plant is considered based on the analytical redundancy approach. Due to mixed dynamics, the modified extended Kalman filter is used for designing the detection filters. These analytical algorithms are housed at the low levels of abstraction of a hierarchical knowledge structure. The knowledge at the higher levels is compiled and suggests a situation-specific filter to be employed for fault diagnostic resolution. Such an integrated approach (analytical and knowledge-based redundancy) reduces the computational complexity of the analytical algorithms and increases the effectiveness of the knowledge-based system.

In the following, first the modified extended Kalman filter algorithm is presented and then the individual filters are formulated. To illustrate the application of the modified algorithm, two typical filters are described in detail.

Nonlinear filtering for systems with coupled static and dynamic models

Different nonlinear techniques for solving the problem of state estimation are available (Anderson and Moore, 1979; Sorenson, 1985) and a short survey of the recursive state estimation techniques is given by Misawa and Hendrick (1988). Among these techniques, the Extended Kalman Filter (EKF) method is widely used by most investigators to solve practical problems (Sorenson, 1985). Therefore, this suboptimal filter is used in the design of state and parameter estimators. From the fault detection viewpoint, it is important to consider the application of the Extended Kalman filter algorithm to the joint parameter and state estimation for systems with coupled static and dynamic models.

In a discrete-time framework, the model of a general stochastic system can be described mathematically by the following equations:

$$x_d(t) = f_d[t, x_d(t-1), x_s(t-1); \theta(t-1)] + w_d \tag{32}$$

$$0 = f_s[t, x_d(t), x_s(t); \theta(t)] + w_s \tag{33}$$

$$y(t) = h[t, x_d(t), x_s(t); \theta(t)] + v(t) \tag{34}$$

where Eqs. 32 and 33 describe the dynamic and static models, respectively, and Eq. 34 is the measurement model, and

$v(t)$ = additive measurement noise
$w(t)$ = additive process noise
$x_d(t)$ = system state with slow dynamics
$x_s(t)$ = system state with fast dynamics
$y(t)$ = output vector (observable signals)
$\theta(t)$ = $[c^T(t)\ d_u^T(t)]$; c and d_u are physical coefficients and unmeasured disturbances, respectively

To cope with time-varying parameters, we postulate that the true parameter vector θ varies according to a random walk model as

$$\theta(t) = \theta(t-1) + w_\theta \tag{35}$$

To tackle the joint state and parameter estimation problem, the augmented state vector z is defined as

$$z^T(t) = [x_d^T(t) \quad x_s^T(t) \quad \theta^T(t)] \tag{36}$$

Upon using the nonlinear Kalman filter approach (Bryson and Ho, 1974; Anderson and Moore, 1979), the estimate of $z(t)$ based on the sequence of measurements $y^t = \{y(0), y(1), \ldots y(t)\}$ for the augmented stochastic system described by Eqs. 32-34, is given by the sequential use of the following recursive algorithm (Fathi et al., 1992)

$$\hat{z}(t) = \bar{z}(t) + K(t)[y(t) - h(t, \bar{z}(t))] \tag{37}$$

$$K(t) = P(t)H^T(t)Q_v^{-1}(t) \tag{38}$$

$$P(t) = M(t) - M(t)H^T(t)[H(t)M(t)H^T(t) + Q_v(t)]^{-1}H(t)\mathbf{M}(t) \tag{39}$$

$$M(t) = F(t-1)P(t-1)F^T(t-1) + Q_w(t-1) \tag{40}$$

$$M(0) = M_0 \tag{41}$$

$$\bar{z}(0) = z_0 \tag{42}$$

where

$$H(t) = \frac{\partial h(t, \bar{z}(t))}{\partial z};\ K(t) = \text{Kalman gain}$$

$M(t) = E\{(z(t) - \bar{z}(t))(z(t) - \bar{z}(t))^T\}$; error covariance matrix prior to measurements at time t

$P(t) = E\{(z(t) - \hat{z}(t))(z(t) - \hat{z}(t))^T\}$; error covariance matrix after measurements at time t

Q_v = measurement error covariance matrix

$\bar{z}(t)$ = estimate of $z(t)$ prior to measurements at time t

The submatrices F_{ij} of the matrix $F(t) = \{\vdots F_{ij} \vdots\}$ for $i, j = 1, 2, 3$ are given by:

$$F_{11} = \frac{\partial \hat{f}_d}{\partial x_d} \quad F_{12} = \frac{\partial \hat{f}_d}{\partial x_s} \quad F_{13} = \frac{\partial \hat{f}_d}{\partial \theta}$$

$$F_{21} = -\left(\frac{\partial \bar{f}_s}{\partial x_s}\right)^{-1}\frac{\partial \bar{f}_s}{\partial x_d}\frac{\partial \hat{f}_d}{\partial x_d} \quad F_{22} = -\left(\frac{\partial \bar{f}_s}{\partial x_s}\right)^{-1}\frac{\partial \bar{f}_s}{\partial x_d}\frac{\partial \hat{f}_d}{\partial x_s}$$

$$F_{23} = -\left(\frac{\partial \bar{f}_s}{\partial x_s}\right)^{-1}\left(\frac{\partial \bar{f}_s}{\partial x_d}\frac{\partial \hat{f}_d}{\partial \theta} + \frac{\partial \bar{f}_s}{\partial \theta}\right)$$

$$F_{31} = 0 \quad F_{32} = 0 \quad F_{33} = I \tag{43}$$

The submatrices Q_{ij} of the matrix $Q_w(t) = \{\vdots Q_{ij} \vdots\}$ for $i, j = 1, 2, 3$ are defined by the following expressions:

$$Q_{11} = Q_d \quad Q_{12} = -Q_d\left(\frac{\partial \bar{f}_s}{\partial x_d}\right)^T\left(\frac{\partial \bar{f}_s}{\partial x_s}\right)^{-T} \quad Q_{13} = 0$$

$$Q_{21} = -\left(\frac{\partial \bar{f}_s}{\partial x_s}\right)^{-1}\frac{\partial \bar{f}_s}{\partial x_d}Q_d \quad Q_{23} = -\left(\frac{\partial \bar{f}_s}{\partial x_s}\right)^{-1}\frac{\partial \bar{f}_s}{\partial \theta}Q_\theta$$

$$Q_{22} = \left(\frac{\partial \bar{f}_s}{\partial x_s}\right)^{-1}\left[Q_s + \left(\frac{\partial \bar{f}_s}{\partial x_d}\right)Q_d\left(\frac{\partial \bar{f}_s}{\partial x_d}\right)^T + \left(\frac{\partial \bar{f}_s}{\partial \theta}\right)Q_\theta\left(\frac{\partial \bar{f}_s}{\partial \theta}\right)^T\right]\left(\frac{\partial \bar{f}_s}{\partial x_s}\right)^{-T}$$

$$Q_{31} = 0 \quad Q_{32} = -Q_\theta\left(\frac{\partial \bar{f}_s}{\partial \theta}\right)^T\left(\frac{\partial \bar{f}_s}{\partial x_s}\right)^{-T} \quad Q_{33} = Q_\theta \tag{44}$$

where

$$\frac{\partial \bar{f}_s}{\partial x} = \frac{\partial f_s}{\partial z}\bigg|_{z = \bar{z}_{(t-1)}} \qquad \frac{\partial \hat{f}_d}{\partial z} = \frac{\partial f_d}{\partial z}\bigg|_{z = \hat{z}_{(t)}}$$

Q_d, Q_s, and Q_θ are covariances of process noises in dynamic, static, and parameter models, respectively, and $(\cdot)^{-T}$ denotes the transposed inverse of $(\cdot)$.

In general, the structure of the modified extended Kalman filter algorithm is the same as in the case of the extended Kalman filter for nonlinear dynamic models. The main differences are in the computation of the system matrix F and the generalized system noise covariance matrix Q_w which include appropriate static-dynamic interaction terms.

Compensation of the extended Kalman filter

The extended Kalman filter can respond properly to parameter variations if they are relatively slow with time (Sorenson, 1985). However, in fault detection systems, variations of unknown parameters can be abrupt and in addition can occur any time. Since the estimation error covariance matrix for the unknown parameters in the extended Kalman filter algorithms decreases monotonically, the filter cannot effectively estimate the parameter changes that occur later in time. To prevent such filter degradation, several techniques have been proposed in which the monotonical decrease of the filter gain is prevented by additional conditions (Jazwinski, 1970; Sriyananda, 1972; Yoshimura et al., 1979).

To avoid filter degradation in estimating faulty parameters, the method of Yoshimura et al. (1979) is adapted. In this technique, the condition that needs to be checked is

$$|\theta_i^n - \hat{\theta}_i(t)| > d[M_{\theta_i}(t+1)]^{1/2} \tag{45}$$

where θ_i^n and $\hat{\theta}_i(t)$ are the nominal values and estimates of θ_i, respectively, $M_{\theta_i}(t)$ are the error variances of θ_i, and d denotes a positive constant (a typical value is 1.96 corresponding to a 95% confidence level). If the condition in Eq. 45 is satisfied for one or more parameter estimates, then the modified variances $M_{\theta_i}^n(t)$ are redefined as

$$M^m_{\theta_i}(t+1) = [\theta^n_i - \hat{\theta}_i(t)]^2/d^2 \tag{46}$$

and are substituted into the filter equations. In addition, after such modification, new values of θ^n_i are changed as $\theta^n_i = \hat{\theta}_i(t)$.

Detection of changes due to unmodeled phenomena

When a filter is activated by the qualitative/compiled knowledge, it does not imply that the triggered filter models the system behavior properly. Thus, it is essential to determine whether the activated filter tracks the actual system behavior. The suspected fault(s) can then be dismissed or accepted based upon the validity of the filter model.

A variety of statistical tests can be performed on the innovations or residuals to determine the validity of the model used in the filter design. The innovations sequence $\{\epsilon(t)\}$ and its associated covariance matrix $S_\epsilon(t) = E\{\epsilon(t)\epsilon^T(t)\}$ are given by

$$\epsilon(t) = y(t) - h(t, \bar{z}(t)) \tag{47}$$

$$S_\epsilon(t) = H(t)M(t)H^T(t) + Q_v(t) \tag{48}$$

If the filter reflects the actual system behavior properly, the innovations sequence is an independent Gaussian random sequence with zero mean and covariance $S_\epsilon(t)$. However, if a system abnormality occurs due to unmolded phenomena, the statistics of $\epsilon(t)$ change. To monitor the measurement innovations (or residuals), we use the modified Sequential Probability Ratio Test (SPRT) of Chien and Adams (1976).

For each component $\epsilon_i(t)$ of the innovations sequence, the following hypotheses are given:

Null hypothesis (H_o): $\epsilon_i(t)$ is an independent Gaussian random sequence with zero mean and variance $S_{\epsilon_i}(t)$, and

Alternative hypothesis (H_1): $\epsilon_i(t)$ is an independent Gaussian random sequence with mean $a_i(t)$ and variance $S_{\epsilon_i}(t)$.

$S_{\epsilon_i}(t)$ denotes the $(i,i)^{\text{th}}$ component of the covariance matrix $S_\epsilon(t)$, $a_i(t) = a\sqrt{S_{\epsilon_i}(t)}$, and a is a positive constant.

The test statistic of SPRT is defined as the logarithm of the joint likelihood ratio function (LLR),

$$l_i(t) = \ln \frac{p(\epsilon_i(1), \epsilon_i(2), \cdots, \epsilon_i(t) \mid H_1)}{p(\epsilon_i(1)\epsilon_i(2), \cdots, \epsilon_i(t) \mid H_0)} \tag{49}$$

For a sequence of independent Gaussian random variables $\{\epsilon_i(t)\}$, the LLR can be generated recursively as,

$$l_i(t) = l_i(t-1) + a\left[\tilde{\epsilon}_i(t) - \frac{1}{2}a\right] \tag{50}$$

$$l_i(0) = 0 \tag{51}$$

where $\tilde{\epsilon}_i(t) = \epsilon_i(t)/\sqrt{S_{\epsilon_i}(t)}$ is the normalized quantity with mean a and variance 1 (a typical value of a is 1.0). A test for the negative-valued bias is implemented by replacing a with $-a$. The modified LLR of Chien and Adams is determined as

$$l_i^+(t) = \begin{cases} l_i^+(t) & \text{if } l_i^+(t) \geq 0 \\ 0 & \text{if } l_i^+(t) < 0 \end{cases} \tag{52}$$

Then, the decision rule is defined as

$$\begin{aligned} &\text{if } l_i^+(t) > \lambda_s, && \text{choose } H_1 \\ &\text{if } 0 \leq l_i^+(t) \leq \lambda_s, && \text{take another observation} \end{aligned} \tag{53}$$

The upper threshold λ_s can be computed for a specified mean time between false alarms T_{mean},

$$T_{\text{mean}} = \frac{2}{a^2}(e^{\lambda_s} - \lambda_s - 1) \tag{54}$$

or specified error probabilities for false alarms (α) and missed alarms (β),

$$e^{\lambda_s} - \lambda_s - 1 = -\left(B + A\,\frac{e^B - 1}{1 - e^A}\right) \tag{55}$$

where

$$A = \ln\left(\frac{\beta}{1-\alpha}\right) \tag{56}$$

$$B = \ln\left(\frac{1-\beta}{\alpha}\right) \tag{57}$$

For $\alpha = \beta = 0.05$, λ_s is computed to be 4.06.

Local filters design

To design local filters, the system shown in Figure 2 is decomposed into: condensate pump, control valve/condensate line, extraction pipe, deaerator, and controller. The faults considered for detection using the Kalman filter approach are transportation line faults: valve/condensate line flow conductance (C_{eq}), valve/condensate line leak (ω_v), and stream flow rate (ω_e); sensors failures: deaerator level sensor (L), condensate flow sensor (ω_p), and deaerator output flow sensor ($\omega_{d_{\text{out}}}$); gain faults in the controller: proportional gain (k_p) and integral gain (k_I). It should be mentioned that these faults constitute only a portion of the faults considered in the knowledge-based system (see next section). The remaining faults are detected using compiled/qualitative knowledge about the process. In the following, the design problem of local estimators is considered.

For the deaerator level control valve (and the piping associated with low-pressure feedwater heaters), two filters are designed. The augmented state vector and the output vector for these filters are defined as

$$\text{Filter I } z^T = [\omega_p C_{eq}],\ y = [\omega_p] \tag{58}$$

$$\text{Filter II } z^T = [P_p \omega_v],\ y = [P_p] \tag{59}$$

In Filter I, ω_p (the mass-flow rate of water entering valve) is the state variable and C_{eq} (the equivalent conductance) is the unknown parameter while in Filter II, P_p (the pressure of water entering valve) is the state variable and ω_v (the mass-flow rate

of water leaving valve) is the unknown parameter. Filter I simulates a fault model corresponding to a change in conductance (for example, fouling) and Filter II models a fault that manifests itself as a change in flow (for example, leak, flow sensor failure). The state equation in both filters is obtained from the static model given by Eq. 11.

For the extraction pipe, the augmented state vector and the output are defined as

$$z^T = [P_e \omega_e], \qquad y = [P_e] \tag{60}$$

Here, the desired state variable is the steam pressure at the outlet of the extraction pipe and the unknown parameter to be estimated is the steam mass-flow rate. The state equation is obtained by solving Eq. 18 for P_e. This filter simulates a fault model corresponding to a low or high input steam flow to the deaerator.

In the filter considered for the deaerator, the states and outputs are defined as

$$z^T = [h_d P_d \omega_{d_{out}}], \quad y^T = [L\ P_d] \tag{61}$$

h_d and P_d are the state variables described by the discrete version of the dynamic equations that are obtained by transforming Eqs. 21 and 22 through the use of Eqs. 24 and 25. This filter is designed to detect output flow sensor failure (this sensor is in the loop of the deaerator level control system). The faulty mode is indicated by the discrepancy between the estimated and measured quantities.

Another detection filter based on the deaerator model was considered for the level sensor failure. In this model, enthalpy and pressure were defined as states and pressure as the only measured quantity. A linear time-invariant approximation of the model was used to study the observability properties of the state-space model. The enthalpy was found to have very poor observability behavior. This was revealed through examining both the observability matrix and the observability gramian. The alternative is to use an autoregressive moving average model for the level sensor. This is a quite attractive approach which can in general be used for sensor validation at the highest level of trouble-shooting (Yung and Clarke, 1989).

For the controller, the filters are designed according to

$$\text{Filter I } z^T = [O_I k_I], \quad y = [O_T] \tag{62}$$

$$\text{Filter II } z^T = [O_I k_P], \quad y = [O_T] \tag{63}$$

The integrator output, O_I, is the state variable described by the dynamic Eq. 30. The unknown parameters are considered to be the integrator gain, k_I, and the proportional gain, k_P. The measured quantity is the controller output, O_T, which is the sum of proportional and integrator outputs.

To illustrate the application of the modified EKF, two filters that correspond to the valve/ condensate line and the deaerator will be described in detail.

A typical fault of the valve/condensate line is partial plugging which can be detected by the on-line identification of the conductance, C_{eq}. To solve this problem, the process model is expressed as

$$\omega_p = C_{eq}[\rho_{pv}(P_p - P_v) + \rho_{pv}^2 \Delta H_v/144]^{1/2} + w_s \tag{64}$$

$$C_{eq}(t+1) = C_{eq}(t) + w_\theta \tag{65}$$

with the measurement equation

$$y = \omega_p + v \tag{66}$$

where w_s and w_θ are the process and parameter model noises, v is the measurement noise, and t denotes the discrete time points. The process model in Eqs. 64-66 is described by both the static Eq. 64 and the dynamic parameter Eq. 65.

To design the modified EKF in Eqs. 37-44 for the system described by Eqs. 64-66, the static, dynamic, and observation functions take the following form

$$f_d(\cdot) = \mathbf{0}, \quad h(\cdot) = \omega_p$$
$$f_s(\cdot) = C_{eq}[\rho_{pv}(P_p - P_v) + \rho_{pv}^2 \Delta H_v/144]^{1/2} - \omega_p \tag{67}$$

Using the above model description, the system matrix F in Eq. 43 reduces to

$$F = \begin{bmatrix} 0 & f_{12} \\ 0 & 1 \end{bmatrix} \tag{68}$$

where

$$f_{12} = -\left(\frac{\partial \bar{f}_s}{\partial \omega_p}\right)^{-1} \frac{\partial \bar{f}_s}{\partial C_{eq}}$$

Similarly, the generalized system noise covariance matrix Q_w in Eq. 44 reduces to a (2×2) matrix whose elements are

$$q_{11} = \left(\frac{\partial \bar{f}_s}{\partial \omega_p}\right)^{-1} \left[Q_s + \frac{\partial \bar{f}_s}{\partial C_{eq}} Q_\theta \frac{\partial \bar{f}_s}{\partial C_{eq}} \right] \left(\frac{\partial \bar{f}_s}{\partial \omega_p}\right)^{-1}$$
$$q_{12} = -\left(\frac{\partial \bar{f}_s}{\partial \omega_p}\right)^{-1} \frac{\partial \bar{f}_s}{\partial C_{eq}} Q_\theta$$
$$q_{21} = -Q_\theta \left(\frac{\partial \bar{f}_s}{\partial C_{eq}}\right) \left(\frac{\partial \bar{f}_s}{\partial \omega_p}\right)^{-1} \qquad q_{22} = Q_\theta. \tag{69}$$

Q_θ and Q_s are scalars and denote variances of parameter and static model noises, respectively. From Eq. 67, the derivates of $f_s(\cdot)$ with respect to ω_p and C_{eq} are given as

$$\frac{\partial f_s}{\partial \omega_p} = -1, \quad \frac{\partial f_s}{\partial C_{eq}} = [\rho_{pv}(P_p - P_v) + \rho_{pv}^2 \Delta H_v/144]^{1/2} \tag{70}$$

From the measurement Eq. 66, we also have

$$H = [1\ 0] \tag{71}$$

To identify the deaerator output flow sensor failure, the deaerator input-output model is used to estimate the output flow rate. The deaerator model consists of differential equations for the bulk density (ρ_d) and the bulk internal energy (u_d). Neither ρ_d nor u_d are measurable; however, the deaerator

pressure, which is implicitly related to ρ_d and u_d, is a measured quantity. Furthermore, the other measured variable is the level in the storage tank which is related to the deaerator pressure and enthalpy through Eq. 27. To formulate the deaerator filter, the dynamic equations for ρ_d and u_d are first transformed into those for h_d (bulk enthalpy) and P_d (pressure).

Through the use of Eqs. 24 and 25, Eqs. 21 and 22 are transformed to the following form for the bulk specific enthalpy, h_d, and the deaerator pressure, P_d,

$$\frac{dh_d}{dt} = [\omega_{d_{in}} h_{d_{in}} - \omega_{d_{out}} h_{d_{out}} + (-h_d + \gamma/\alpha_p)(\omega_{d_{in}} - \omega_{d_{out}})]/[V_{tn}(\rho_d + \gamma\alpha_h/\alpha_p)] \quad (72)$$

$$\frac{dP_d}{dt} = (\omega_{d_{in}} - \omega_{d_{out}})/(V_{tn}\alpha_p) - (\alpha_h/\alpha_p)\frac{dh_d}{dt} \quad (73)$$

where

$$\alpha_h = \left.\frac{\partial \rho_d}{\partial h_d}\right|_{P_d \text{ constant}}, \quad \alpha_p = \left.\frac{\partial \rho_d}{\partial P_d}\right|_{h_d = \text{constant}}, \quad V_{tn} = 3{,}600\ V_t$$

To formulate the failure detection system, the time-continuous nonlinear deaerator model should be discretized. Using the forward discretization method, the discrete process model with w_{d_1} and w_{d_2} as process noises are

$$h_d(t+1) = h_d(t) + \Delta t\, f_h(t) + w_{d_1} \quad (74)$$

$$P_d(t+1) = P_d(t) + \Delta t(\omega_{d_{in}}(t) - \omega_{d_{out}}(t))/(V_{tn}\alpha_p(t)) - \Delta t(\alpha_h(t)/\alpha_p(t))f_h(t) + w_{d_2} \quad (75)$$

where

$$f_h(t) = [\omega_{d_{in}}(t)h_{d_{in}}(t) - \omega_{d_{out}}(t)h_{d_{out}}(t) + (-h_d(t) + \gamma/\alpha_p(t))(\omega_{d_{in}}(t) - \omega_{d_{out}}(t))]/[V_{tn}(\rho_d(t) + \gamma\alpha_h(t)/\alpha_p(t))]$$

Here, t is used to denote the discrete time points. It is worth to point out that the above mathematical description of the modeled deaerating process is given by a system of highly nonlinear equations with complex two-phase behavior. The additional equations needed include the parameter model

$$\omega_{d_{out}}(t+1) = \omega_{d_{out}}(t) + w_\theta \quad (76)$$

and the measurement equations

$$y_1 = L + v_1 \quad (77)$$

$$y_2 = P_d + v_2 \quad (78)$$

where v_1 and v_2 are measurement noises.

For the dynamic deaerator model Eqs. 74–78, the modified EKF reduces to the nonlinear Kalman filter. Based on the above model definition, the elements of the dynamic function $f_d = [f_1\ f_2]^T$, the static function f_s, and the observation vector h are

$$f_1(\cdot) = h_d + \Delta t\, f_h$$

$$f_2(\cdot) = P_d + \Delta t(\omega_{d_{in}} - \omega_{d_{out}})/(V_{tn}\alpha_p) - \Delta t(\alpha_h/\alpha_p)f_h$$

$$f_s(\cdot) = \mathbf{0}$$

$$h^T(\cdot) = [L\ P_d] \quad (79)$$

Hence, the elements of the matrix F in Eq. 43 are

$$F = \begin{bmatrix} \frac{\partial f_1(\cdot)}{\partial h_d} & \frac{\partial f_1(\cdot)}{\partial P_d} & \frac{\partial f_1(\cdot)}{\partial \omega_{d_{out}}} \\ \frac{\partial f_2(\cdot)}{\partial h_d} & \frac{\partial f_2(\cdot)}{\partial P_d} & \frac{\partial f_2(\cdot)}{\partial \omega_{d_{out}}} \\ 0 & 0 & 1 \end{bmatrix} \quad (80)$$

The derivatives of f_1 and f_2 with respect to h_d, P_d, and $\omega_{d_{out}}$ are given as

$$\frac{\partial f_1(\cdot)}{\partial h_d} = 1 + \Delta t\frac{\partial f_h}{\partial h_d}, \quad \frac{\partial f_1(\cdot)}{\partial P_d} = \Delta t\frac{\partial f_h}{\partial P_d}$$

$$\frac{\partial f_2(\cdot)}{\partial h_d} = -\Delta t\frac{\partial}{\partial h_d}[(\alpha_h/\alpha_p)f_h]$$

$$\frac{\partial f_2(\cdot)}{\partial P_d} = 1 + \Delta t\left[((\omega_{d_{in}} - \omega_{d_{out}})/V_{tn})\frac{\partial \alpha_p^{-1}}{\partial P_d}\right] - \Delta t\frac{\partial}{\partial P_d}[(\alpha_h/\alpha_p)f_h] \quad (81)$$

$$\frac{\partial f_1(\cdot)}{\partial \omega_{d_{out}}} = \Delta t\frac{\partial f_h}{\partial \omega_{d_{out}}}$$

$$\frac{\partial f_2(\cdot)}{\partial \omega_{d_{out}}} = -\Delta t/(V_{tn}\alpha_p) - \Delta t(\alpha_h/\alpha_p)\frac{\partial f_h}{\partial \omega_{d_{out}}}$$

In this case, the generalized system error covariance matrix Q_w Eq. 44 reduces to

$$Q_w = \begin{bmatrix} Q_d & 0 \\ 0 & Q_\theta \end{bmatrix} \quad (82)$$

where Q_d is the covariance matrix of process noises w_{d_1} and w_{d_2}, and Q_θ is the variance of parameter model noise w_θ. Furthermore, the elements of the observation matrix H are

$$H = \begin{bmatrix} \frac{\partial L}{\partial h_d} & \frac{\partial L}{\partial P_d} & 0 \\ 0 & 1 & 0 \end{bmatrix} \quad (83)$$

where Eq. 27 is used to determine $\partial L/\partial h_d$ and $\partial L/\partial P_d$.

Knowledge Base

The following gives a brief description of our knowledge base. Further details can be found in another article (Fathi et al., 1992).

The overall objective in developing a knowledge-based system is to capture both the domain knowledge and the problem-

solving strategy. Thus, an essential element in knowledge-based system development lies in understanding the problem in terms of knowledge, organization of knowledge, and reasoning strategies. Human organizational strategies and conceptual abstractions suggest a hierarchical representation of knowledge (Rasmussen, 1985). The hierarchical structure offers efficient top-down solution procedures for classification-type problems.

An appropriate domain concept for context grouping of diagnostic knowledge in a hierarchical structure is malfunction hypothesis (Chandrasekaran, 1984, 1986). Thus, to provide a necessary general structure for the knowledge base, a malfunction hierarchy is identified for organizing knowledge about the system (Shum et al., 1988; Ramesh et al., 1988). The use of malfunction hypothesis as the conceptual basis for constructing the hierarchy provides an efficient problem-solving framework, allows for a natural decomposition of the domain for focus and control, and supports organized and efficient knowledge-acquisition. In addition, this approach provides a flexible structure for including and efficiently focusing the quantitative considerations of analytical redundancy techniques.

The construction of the malfunction hierarchy involves the identification of functional systems/subsystems in the process. Figure 3 shows the malfunction hierarchy generated using the system knowledge for the condensate-feedwater subsystem of a power plant. Higher levels are related to more general functional segments and physical subsystems and lower levels are related to more specific functional units and physical components. The hierarchical structure allows the decision process to proceed from a high level of generality to a high level of detail.

The diagnostic knowledge employed at the higher nodes of the hierarchy (more general malfunction hypotheses) is compiled while that at the lower nodes (more specific malfunction hypotheses) makes use of estimation-based techniques. In this manner, initially the compiled knowledge is used to rapidly narrow down the solution space and provide diagnostic focus. Then, the filter modules are triggered to resolve and refine the suspected malfunction hypotheses in the reduced and more focused search space. This integrated approach increases the completeness and reliability of the diagnostic system.

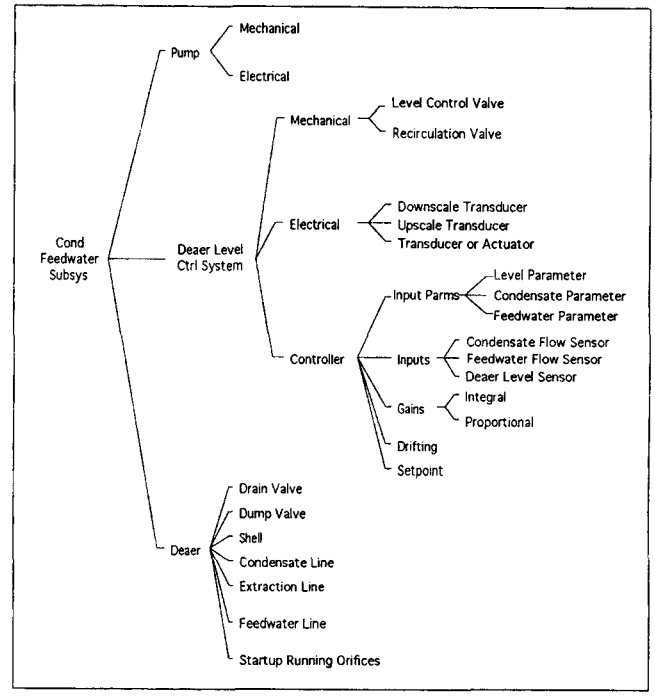

Figure 3. Malfunction hierarchy for condensate-feedwater subsystem.

Implementation

The medium for performing numerical processing tasks such as simulation, statistical analysis, and estimation modules has been identified as MODEL (Model Software, 1991). MODEL is a high-level, object-oriented engineering language that provides solutions for real-time distributed process simulation and control.

Nexpert Object (Neuron Data), a C-based, object-oriented, hybrid tool with a knowledge representation paradigm based on rules and objects constitutes an efficient, integrated medium for our knowledge-based system development. For the condensate-feedwater system, a knowledge base that defines the entities of the system and their characteristics in terms of classes, objects, and properties and contains the problem-solving knowledge in terms of rules has been created. This knowledge base has been developed through preliminary knowledge acquisition based on background knowledge and use of documents such as *Analog/Digital Data Point* and *Instrumentation Logic Diagrams* provided by Public Service Company, and detailed knowledge acquisition based on meetings with plant experts. The mechanism by which events are processed is a dynamic, priority-based scheduling system (agenda). There are several types of inference search mechanisms such as backward chaining, hypothesis forward, semantic gates, context links, and so on with varying priorities (these inference strategies can be disabled or limited in scope globally or locally). One should note that the implementation of a hierarchical knowledge structure provides an additional control strategy beyond those provided by the inference engine.

To provide a graphics-based user interface, MODEL and Nexpert Object are run under Microsoft Windows. The two media are interfaced through the Dynamic Data Exchange (DDE) calls of Microsoft Windows.

Application to Fault Detection

In the current version of the prototype diagnostic system, inputs are simulated. These inputs are statistically tested to determine the plant condition. In the case of detecting an abnormal behavior, the knowledge processing is activated. When a diagnostic focus is obtained, a specific-situation filter is triggered. The filter is run using a window of past and current data including last data transfer.

In this section, some results of the designed local filters are presented. It is reasonable to point out that the faults modeled by the filters constitute a portion of the overall malfunction hierarchy.

A typical fault of the valve/condensate line is partial plugging which can be detected by the on-line identification of the conductance. The filter designed to model this case is defined in Eq. 58. Figure 4 depicts the measured and estimated condensate flow rate and the expected and estimated equivalent

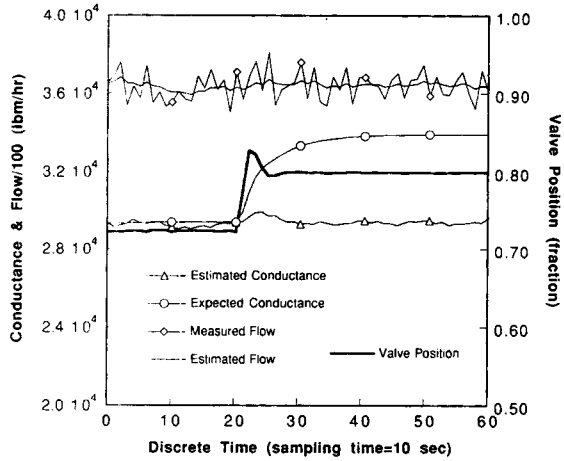

Figure 4. Measured and estimated flow, expected and estimated conductance, and valve position vs. time: valve/condensate line.

conductances when the pipe conductance was reduced by 20 percent after some time had elapsed. The equivalent conductance is a function of valve position. As the flow resistance was increased, the valve opened up in order to prevent the deaerator level from dropping. The expected conductance represents the normal value while the estimated conductance represents the present condition. The fault is determined by examining the normalized deviation between the expected conductance (2.9×10^4) and present value (3.4×10^4). The goodness of the filter tracking the system behavior is manifested by comparing the estimated and measured flow values.

The other example corresponds to the condensate flow sensor failure or a leak in the condensate line. The filter designed to estimate the condensate flow rate is defined in Eq. 59. The results obtained from a test case are represented in Figure 5. The filter is started from a value (4.0×10^6 lb_m/h) that is substantially higher than the actual flow rate (3.65×10^6 lb_m/h). As it is observed, the estimation module quickly determines the correct value of the flow rate. A fault (flow sensor failure or a leak) is detected when the output from the filter deviates significantly from the sensor value (in this case, the starting condition).

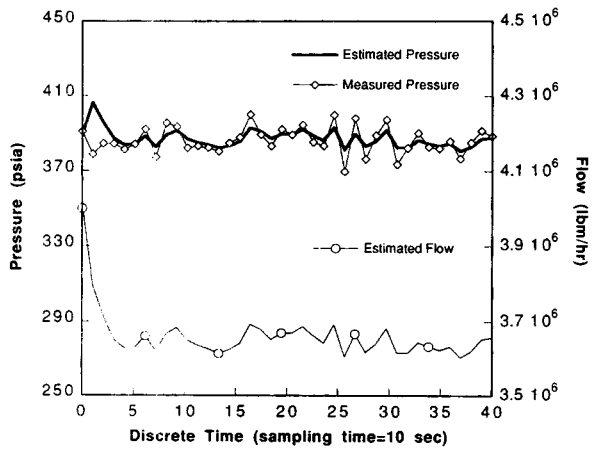

Figure 5. Measured pressure and estimated pressure and flow vs. time: valve/condensate line.

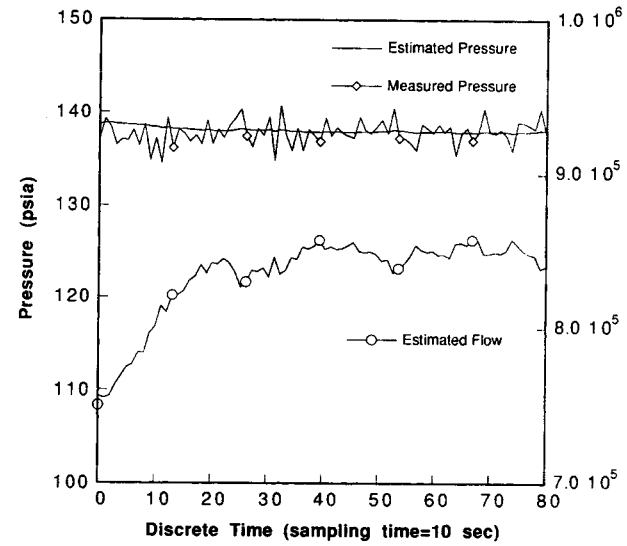

Figure 6. Measured pressure and estimated pressure and flow vs. time: extraction pipe.

The extraction pipe estimation module is to estimate the flow rate of steam entering the deaerator. The steam flow rate is used to determine that the abnormalities detected in the deaerator are due to low (or high) steam flow rates which are caused by some other sources. The estimated and measured pressures at the pipe outlet and the estimated steam flow rate are shown in Figure 6. The initial condition for the flow rate (7.5×10^5 lb_m/h) is significantly lower than the true value (8.5×10^5 lb_m/h). In this case, the actual value is estimated rather quickly and accurately.

The deaerator module is used to estimate the deaerator output flow rate which can then be compared with the sensor value to detect sensor failure. The estimation results for this case are depicted in Figures 7 and 8. In Figure 7, the initial value for the output flow rate (3.5×10^6 lb_m/h) is considerably different than the actual value (4.5×10^6 lb_m/h) while the deaerator pressure and enthalpy values correspond to a steady-state operating condition. In Figure 8, the initial values for the two states ($P_d = 132.0$ psia, $h_d = 328.0$ Btu/lb_m) and the parameter ($\omega_{d_{out}} = 3.5 \times 10^6$ lb_m/h) are different than the existing operating

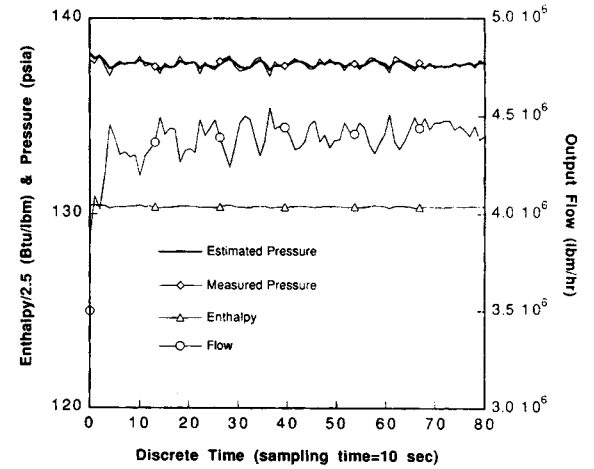

Figure 7. Measured pressure and estimated pressure, enthalpy, and flow vs. time: deaerator.

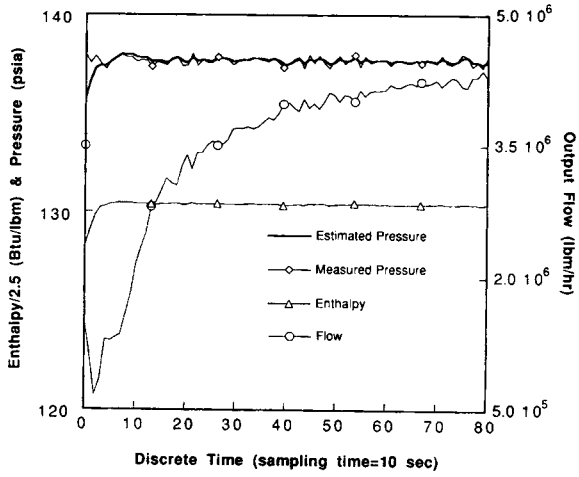

Figure 8. Measured pressure and estimated pressure, enthalpy, and flow vs. time: deaerator.

values ($P_d = 137.7$ psia, $h_d = 325.9$ Btu/lb$_m$, $\omega_{d_{out}} = 4.5 \times 10^6$ lb$_m$/h). As it is observed, the states quickly approach the actual values while the flow is first underestimated but then rather quickly approaches its correct value. In both cases, the estimation results are good and within reasonable accuracy. It is important to point out that the behavior of this module with respect to parameter estimation is sensitive to measured input and output noises. This problem was alleviated by prefiltering the measurement signals prior to the use in this module.

Two controller modules have been designed to estimate the proportional gain (k_p) and the integral gain (k_I). We should note that these parameters can be estimated only when the system undergoes some dynamic behavior. For the results shown in Figures 9 and 10, the dynamics were introduced by changing the level set point from 120 in. to 115 and 114 in., respectively. The two cases presented correspond to a change in k_I from its nominal value of 0.05 to 0.1 and 0.02. As it is seen, good detection accuracies of the abrupt changes of k_I are attained. It is interesting to note that the controller output signals are similar while the abrupt changes in either direction are correctly detected. The result for the proportional gain is shown in Figure 11. The value of k_p had been changed from

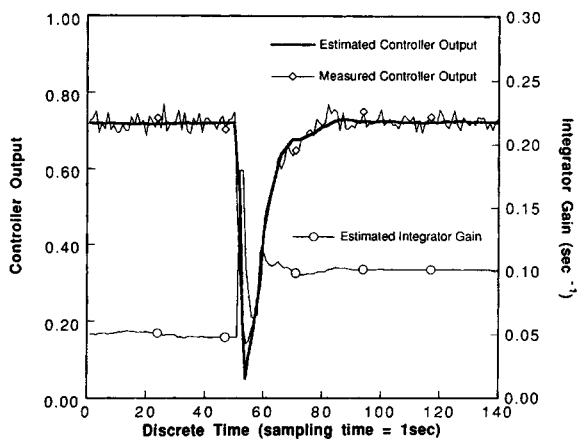

Figure 9. Measured controller output and estimated controller output and integrator gain: controller.

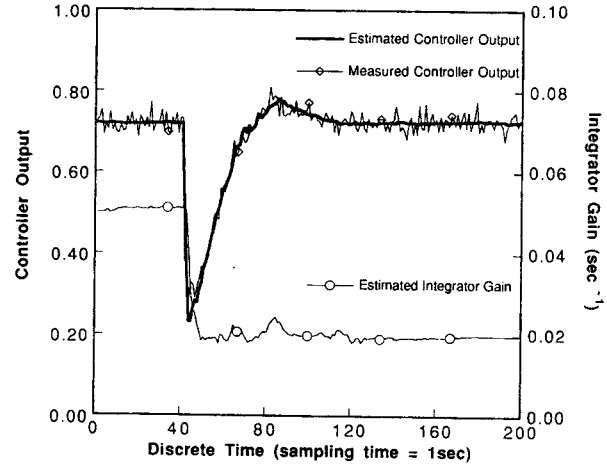

Figure 10. Measured controller output and estimated controller output and integrator gain: controller.

its nominal value of 0.1 to 0.05 prior to the level set point change of 121 to 119 in. The estimation accuracy of this abrupt change is reasonably good. The problem in estimating k_p accurately, without uncertainty, can be attributed to its sensitivity to the noise in the input error signal to the controller.

Conclusions

We have presented a diagnostic methodology in which the symbolic reasoning of knowledge-based systems techniques is integrated with quantitative analysis of analytical redundancy methods. Such an integrated approach (analytical and knowledge-based redundancy) reduces the computational complexity of the analytical algorithms and increases the effectiveness of the knowledge-based system. Our main emphasis in this article has been the design of local state and parameter estimation modules for fault detection and isolation which can then be used in the context of a knowledge-based system. The numerical experiments implemented using the condensate-feedwater subsystem of a power plant demonstrated the

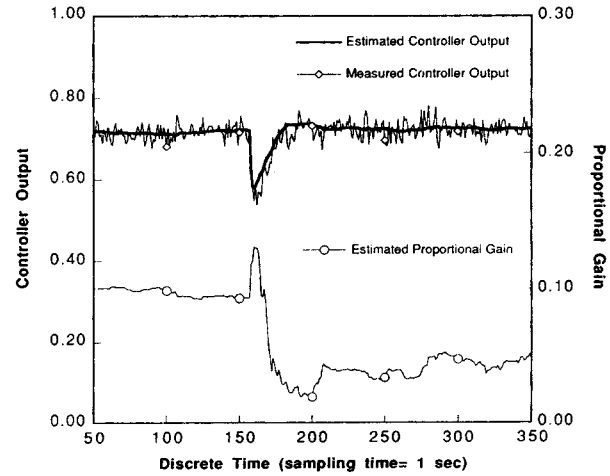

Figure 11. Measured controller output and estimated controller output and proportional gain: controller.

effectiveness of the approach for fault detection in process plants. The analytical redundancy algorithm has been very successful in estimating both measured and unmeasured dynamic states, static states, and system parameters using available measurements.

Notation

a = a positive constant
c = physical coefficients
C_{eq} = equivalent conductance (valve and condensate pipe)
C_f = extraction pipe conductance
C_p = condensate pipe conductance
C_v = valve conductance
$C_{v_{max}}$ = valve maximum conductance
d_u = unmeasured disturbances
D = diameter of deaerator storage tank, in. (mm)
h_c = enthalpy of condensate water entering pump, Btu/lb_m (kJ/kg)
h_d = bulk specific enthalpy of fluid in deaerator, Btu/lb_m (kJ/kg)
$h_{d_{in}}$ = enthalpy of feedwater and steam entering deaerator, Btu/lb_m (kJ/kg)
$h_{d_{out}}$ = enthalpy of fluid leaving deaerator, Btu/lb_m (kJ/kg)
h_e = enthalpy of steam leaving extraction pipe, Btu/lb_m (kJ/kg)
h_p = enthalpy of water leaving pump, Btu/lb_m (kJ/kg)
h_s = enthalpy of steam entering extraction pipe, Btu/lb_m (kJ/kg)
h_v = enthalpy of water leaving valve, Btu/lb_m (kJ/kg)
J = power required by pump, hp (kW)
k_1, k_2, k_3 = constant parameters
k_a = gain on antireset windup
k_I = integrator gain (s^{-1})
k_P = proportional gain
$l_i(t)$ = likelihood ratio function
$l_i^+(t)$ = modified likelihood ratio function
L = liquid level in deaerator in. (mm)
L_m = deaerator level measured in. (mm)
L_s = deaerator level set point in. (mm)
$M(t)$ = error covariance matrix prior to measurements at t
$M_{\theta_i}(t)$ = error variance of θ_i prior to measurements at t
$M^m_{\theta_i}(t)$ = modified error variance of θ_i prior to measurements at t
N = pump speed, rpm
O_h = higher limit on controller output
O_I = integrator output (fraction)
O_l = lower limit on controller output
O_P = proportional output (fraction)
O_T = controller output
P_{bfps} = pressure at boiler feed pump suction, psia (kPa)
P_c = pressure of condensate water entering pump, psia (kPa)
P_d = pressure in deaerator, psia (kPa)
P_e = pressure of steam leaving extraction pipe, psia (kPa)
P_p = pressure of water leaving pump, psia (kPa)
P_s = pressure of steam entering extraction pipe, psia (kPa)
$P(t)$ = error covariance matrix after measurements at t
P_v = pressure of water leaving valve, psia (kPa)
Q_d, Q_s, Q_θ = process noise covariances in dynamic, static, and parameter models, respectively
Q_p = pump volumetric flow rate, gpm (L/s)
Q_v = measurement error covariance matrix
$S_\epsilon(t)$ = innovations covariance matrix
$T_{d_{out}}$ = temperature of fluid leaving deaerator, °F(°C)
T_e = temperature of steam leaving pipe, °F(°C)
T_{mean} = mean time between false alarms
T_p = temperature of water leaving pump, °F(°C)
T_v = temperature of water leaving valve, °F(°C)
u_d = bulk specific internal energy of fluid in deaerator, Btu/lb_m (kJ/kg)
$v(t)$ = additive measurement noise
V_s = volume of storage tank, ft^3 (m^3)
V_t = total volume of deaerating and storage tanks, ft^3 (m^3)
ω_c = mass flow rate of condensate water, lb_m/h (kg/h)
w_d = additive process noise in dynamic model
$\omega_{d_{in}}$ = mass flow rate of feedwater and steam entering deaerator, lb_m/h (kg/h)
$\omega_{d_{out}}$ = mass flow rate of fluid leaving deaerator, lb_m/h (kg/h)
ω_e = mass flow rate of steam leaving extraction pipe, lb_m/h (kg/h)
ω_p = mass flow rate of water leaving pump, lb_m/h (kg/h)
w_s = additive process noise in static model
ω_s = mass flow rate of steam entering extraction pipe, lb_m/h, (kg/h)
ω_v = mass flow rate of water leaving valve, lb_m/h (kg/h)
w_θ = process noise in parameter model
$x_d(t)$ = system state with slow dynamics
$x_s(t)$ = system state with fast dynamics
$y(t)$ = output vector (observable signals)
$z(t)$ = augmented state vector
$\hat{z}(t)$ = estimate of $z(t)$ after measurements at t
$\bar{z}(t)$ = estimate of $z(t)$ prior to measurements at t

Greek letters

α = error probability for false alarms
β = error probability for missed alarms
ΔH_{db} = elevation drop from deaerator to boiler feed pump, ft (m)
ΔH_p = pump developed head, ft (m) of water
ΔH_{se} = elevation difference between upstream and downstream segments of extraction pipe, ft (m)
ΔH_v = difference in elevation between inlet and outlet of valve, ft (m)
ϵ = control error signal
$\epsilon(t)$ = innovations
γ = conversion factor equivalent to 0.1851 (Btu·in.^{2})/(lb_f·ft^3)
λ_s = upper threshold for modified SPRT
ρ_c = density of condensate water entering pump, lb_m/ft^3 (kg/m^3)
ρ_d = bulk density of fluid in deaerator, lb_m/ft^3 (kg/m^3)
$\rho_{d_{out}}$ = density of fluid leaving deaerator, lb_m/ft^3 (kg/m^3)
ρ_e = density of steam leaving pipe, lb_m/ft^3 (kg/m^3)
ρ_f = density of saturated liquid in deaerator, lb_m/ft^3 (kg/m^3)
ρ_g = density of saturated vapor in deaerator, lb_m/ft^3 (kg/m^3)
ρ_p = density of water leaving pump, lb_m/ft^3 (kg/m^3)
ρ_{pv} = average of upstream and downstream fluid densities for valve, lb_m/ft^3 (kg/m^3)
ρ_{se} = average of downstream and upstream fluid densities for extraction pipe, lb_m/ft^3 (kg/m^3)
ρ_v = density of water leaving valve, lb_m/ft^3 (kg/m^3)
$\theta(t)$ = unknown parameter vector
θ_i^n = ith parameter nominal value
$\hat{\theta}_i$ = ith parameter estimate
Υ = valve position (fraction)

Literature Cited

Anderson, B. D. O., and J. B. Moore, *Optimal Filtering*, Prentice-Hall, Englewood Cliffs, NJ (1979).

Basseville, M., "Detecting Changes in Signals and Systems. A Survey," *Automatica*, 24(3), 309 (1988).

Basseville, M., and A. Benveniste, eds., *Detection of Abrupt Changes in Signals and Dynamical Systems*, Lecture Notes on Control and Information Sciences, M. Thomas and W. Wyner, eds., 77, Springer-Verlag, New York (1986).

Bryson, A. E., and Y. Ho, *Applied Optimal Control*, Hemisphere, New York (1975).

Chandrasekaran, B., "Expert Systems: Matching Techniques to

Tasks," *Artificial Intelligence in Business*, W. Reitman, ed., Ablex Publishing (1984).
Chandrasekaran, B., "Generic Tasks in Knowledge-based Reasoning: High-level Building Blocks for Expert System Design," *IEEE Expert*, **1**(3), 23 (1986).
Chien, T. T., and M. B. Adams, "A Sequential Failure Detection Technique and its Application," *IEEE Trans. on Automatic Control*, **AC-21**, 750 (1976).
Fathi, Z., W. F. Ramirez, and O. Aarna, "A Joint State and Parameter Estimator for Systems with Coupled Fast and Slow Dynamic Modes," AIChE Meeting, Los Angeles (Nov. 17–22, 1991); *Optimal Control Appl. & Methods*, **13** (1992).
Fathi, Z., W. F. Ramirez, A. P. Tavares, G. Gilliland, and J. Korbicz, "A Knowledge-based System with Embedded Estimation Components for Fault Detection and Isolation in Process Plants," IFAC Symposium on On-Line Fault Detection and Supervision in the Chemical Process Industries, Newark, DE, p. 32 (Apr. 22-24, 1992).
Frank, P. M., "Fault Diagnosis in Dynamic Systems Using Analytical and Knowledge-based Redundancy. A Survey and Some New Results," *Automatica*, **26**(3), 459 (1990).
Gertler, J., "Analytical Redundancy Methods in Fault Detection and Isolation," *Proceedings of the IFAC/IMACS Symposium on Fault Detection, Supervision and Safety for Technical Processes*, SAFEPROCESS '91, Baden-Baden, Germany, p. 9 (Sept. 10–13, 1991).
Gertler, J., and D. Singer, "A New Structural Framework for Parity Equation-based Failure Detection and Isolation," *Automatica*, **26**(2), 381 (1990).
Halme, A., and J. Selkäinaho, "An Adaptive Filtering Based Method to Detect Sensor/Actuator Faults," IFAC Kyoto Workshop on Fault Detection and Safety in Chemical Plants, Kyoto, Japan, p. 158 (Sept. 28–Oct. 1, 1986).
Hengy, D., and P. M. Frank, "Component Failure Detection Via Nonlinear State Observers," IFAC Kyoto Workshop on Fault Detection and Safety in Chemical Plants, Kyoto, Japan, p. 153 (Sept. 28–Oct. 1, 1986).
Himmelblau, D. M., *Fault Detection and Diagnosis in Chemical and Petrochemical Processes*, Chemical Engineering Monograph 8, Elsevier Scientific, Amsterdam (1978).
Himmelblau, D. M., "Fault Detection and Diagnosis—Today and Tomorrow," IFAC Kyoto Workshop on Fault Detection and Safety in Chemical Plants, Kyoto, Japan, p. 95 (Sept. 28–Oct. 1, 1986).
Isermann, R., "Process Fault Detection Based on Modeling and Estimation Methods—A Survey," *Automatica*, **30**, 387 (1984).
Jazwinski, A. H., *Stochastic Processes and Filtering Theory*, Academic Press, New York (1970).
Johannsen, G., and J. L. Alty, "Knowledge Engineering for Industrial Experts Systems," *Automatica*, **27**(1), 97 (1991).
Jones, H. L., *Failure Detection in Linear Systems*, PhD Thesis, MIT, Cambridge, MA (1973).
Korbicz, J., Z. Fathi, and W. F. Ramirez, "State Estimation Schemes for Fault Detection and Diagnosis in Dynamic Systems," *Applied Math. & Computer Sci.*, **1**(1), 83 (1991). Zielona Góra, Poland: Higher College of Engineering Publishing House.
Laparo, K. A., M. R. Buchner, and K. S. Vasudeva, "Leak Detection in an Experimental Heat Exchanger Process: A Multiple Model Approach," *IEEE Trans. Automat. Control*, **36**(2), 167 (1991).
Mehra, R. K., and J. Peschon, "An Innovations Approach to Fault Detection and Diagnosis in Dynamic Systems," *Automatica*, **7**, 637 (1971).
Model Software, Solutions for Real Time Simulation and Control, 52 Curtis Court, Broomfield, CO.
Miller, T., R. S. Sutton, and P. J. Werbos, *Neural Networks for Control*, MIT Press, Cambridge, MA (1990).
Misawa, E. A., and J. K. Hedrick, "Nonlinear Observers: A State-of-the-Art Survey," In J. Benstsman and S. M. Joshi, eds., *Recent Advances in Control of Nonlinear and Distributed Parameter Systems, Robust Control, and Aerospace Control Applications*, American Society of Mechanical Engineers, p. 59 (1988).
Naidu, S. R., E. Zafiriou, and T. J. McAvoy, "Use of Neural Networks for Sensor Failure Detection in a Control System," *IEEE Control Systems Magazine*, **10**(3), 49 (1990).
Neuron Data, 444 High Street, Palo Alto, CA.
Park, S. W., and D. M. Himmelblau, "Fault Detection and Diagnosis Via Parameter Estimation in Lumped Dynamic Systems," *Indus. Engr. Chem. Process Des. Develop.*, **22**, 482 (1983).
Patton, R., and J. Chen, "A Review of Parity Space Approaches to Fault Diagnosis," *Proceedings of the IFAC/IMACS Symposium on Fault Detection, Supervision and Safety for Technical Processes*, SAFEPROCESS '91, Baden-Baden, Germany, p. 239 (Sept. 10–13, 1991).
Patton, R., P. Frank, and R. Clark, *Fault Diagnosis in Dynamic Systems. Theory and Applications*, Prentice Hall, New York (1989).
Pau, L. F., *Failure Diagnosis and Performance Maintenance*, Marcel Dekker, New York (1981).
Ramesh, T. S., S. K. Shum, and J. F. Davis, "A Structured Framework for Efficient Problem Solving in Diagnostic Expert Systems," *Computers and Chem. Eng.*, **12**(9/10), 891 (1988).
Rasmussen, J., "The Role of Hierarchical Knowledge Representation in Decisionmaking and System Management," *IEEE Transactions on Systems, Man, and Cybernetics*, **SMC-15**(2), 234 (1985).
Shum, S. K., J. F. Davis, W. F. Punch III, and B. Chandrasekaran, "An Expert System Approach to Malfunction Diagnosis in Chemical Plants," *Computers & Chem. Eng.*, **12**(1), 27 (1988).
Sorenson, H. W., ed., *Kalman Filtering: Theory and Application*, IEEE Press, New York (1985).
Sriyananda, H., "A Simple Method for the Control of Divergence in Kalman Filter Algorithms," *Int. J. Control*, **16**(6), 1101 (1972).
Tzafestas, S. G., ed., *Knowledge-Based System Diagnosis, Supervision and Control*, Plenum, New York (1989).
Watanabe, K., and D. M. Himmelblau, "Fault Diagnosis in Nonlinear Chemical Processes, Part 1—Theory," *AIChE J.*, **29**, 243 (1983a).
Watanabe, K., and D. M. Himmelblau, "Fault Diagnosis in Nonlinear Chemical Processes, Part 2—Application to a Chemical Reactor," *AIChE J.*, **29**, 250 (1983b).
Watanabe, K., and D. M. Himmelblau, "Instrument Fault Detection in Systems with Uncertainties," *Int. J. Syst. Sci.*, **13**(2), 137 (1982).
Willsky, A. S., "A Survey of Design Methods for Fault Detection," *Automatica*, **12**, 601 (1976).
Willsky, A. S., and H. L. Jones, "A Generalized Likelihood Ratio Approach to State Estimation in Linear Systems Subject to Abrupt Changes," *Proc. IEEE Conference on Decision and Control*, Phoenix, Arizona, p. 846 (1974).
Willsky, A. S., and H. L. Jones, "A Generalized Likelihood Ratio Approach to the Detection and Estimation of Jumps in Linear Systems," *IEEE Trans. on Automatic Control*, **AC-21**, 108 (1976).
Willsky, A. S., J. J. Deyst, and B. S. Crawford, "Adaptive Filtering and Self-test Methods for Failure Detection and Compensation," *Proc. JACC*, Austin, Texas, p. 637 (June 19–21, 1974).
Willsky, A. S., J. J. Deyst, and B. S. Crawford, "Two Self-test Methods Applied to an Inertial System Problem," *J. Spacecr. Rockets*, **12**(7), 434 (1975).
Wunnenberg, J., and P. M. Frank, "Dynamic Model-based Incipient Fault Detection Concept for Robot," *Proc. IFAC World Congress*, Tallinn, Estonia, USSR, p. 1420 (1990).
Yao, S. C., and E. Zafiriou, "Control System Sensor Failure Detection Via Networks of Localized Receptive Fields," *Proc. Amer. Control Conf.*, San Diego, CA, **3**, p. 2472 (May 23–25, 1990).
Yoshimura, T., K. Watanabe, K. Konishi, and T. Soeda, "A Sequential Detection Approach and the Identification of Failure Parameters," *Int. J. Systems Sci.*, **10**, 827 (1979).
Yung, S. K., and D. W. Clarke, "Local Sensor Validation," *Measurements and Control*, **22**, 132 (1989).

Manuscript received Jan. 27, 1992, and revision received July 16, 1992.